Development of SH-SAW Sensors
for measurement of the properties of protein solutions

Yongrae Roh*[a], Yongjun Kwon[a], Kyungho Kim[b], Kwangnak Koh[c] and Jaeho Kim[d]

[a]School of Mechanical Engineering, Kyungpook National University, Taegu 702-701, Korea
[b] Samsung Advanced Institute of Technology, P.O.Box 111, Suwon 440-600, Korea
[c]Department of Chemical Engineering, Kyungpook National University, Taegu 702-701, Korea
[d]Department of Molecular Science and Technology, Ajou University, Suwon 442-749, Korea

ABSTRACT

We developed new surface acoustic wave (SAW) sensors to measure the properties of protein solutions applying a particular organic thin film on the delay line of transverse type SAW devices. Each delay line is configured as an oscillator. The delay line for a sensing channel is coated with a gold film on which an antibody layer is immobilized by protein A. The sensing delay line selectively adsorbs antigens when exposed to a protein solution, which results in phase delay changes due to the mass loading effects induced by the adsorbed antigens. The other delay line is uncoated for use as a stable reference. The relative change in the frequency of the two oscillators is monitored to measure the concentration of the antigens. Sensor properties investigated include selectivity, sensitivity, response time and stability in response to the antigen concentration as well as the viscosity and electrical conductivity of the protein solution.
Keywords: LiTaO3 single crystals, SH-SAW sensor, protein, oscillator

1. INTRODUCTION

A surface acoustic wave (SAW) is very sensitive to its environment. Here, the environment encompasses any variable surrounding the SAW, such as temperature, humidity and forces. When a SAW is exposed to these variables, it shows a great deal of velocity change in measure with the variable changes. When a SAW sensor is configured as a feedback oscillator, the velocity change of a SAW leads to corresponding oscillation frequency change. If the environment is liquid, the SAW can respond to the properties associated with the liquid. However, in underwater environment, the SAW is likely to leak its energy into the liquid, which leads to poor performance of the sensor. Based on these characteristics of the SAW, we developed SH-SAW sensors that can show stable response with good sensitivity for immersion applications [1]. The sensor consists of twin SAW delay lines operating at 100 MHz, a sensitive channel and a reference channel, fabricated on 36 degrees rotated Y-cut X-propagation $LiTaO_3$ piezoelectric single crystals. By virtue of the particular crystal cut and wave propagation direction, the sensor is made to launch a SAW having its displacement polarization in shear horizontal (SH) direction. Figure 1 is a schematic diagram illustrating the propagation of the SH-SAW and a SV- (shear vertical) SAW like the well-known Rayleigh wave. Compared with the Rayleigh waves widely employed for conventional SAW sensors, the SH-SAW shows little attenuation in propagation under liquid loading environment and thus leads to better signal to noise ratio and system stability. Recently, there is a great need for very sensitive micro- or nano-scale sensors that can respond to the effects of various chemical or biological materials such as DNA and protein cells. The SAW sensor in this work can be one of the candidates to meet such demands [2,3].

2. CHARACTERISTICS OF A SH-SAW DEVICE

In order to confirm the suitability of the SH-SAW for underwater sensing applications, preliminary experiments and

numerical simulations were performed. Figure 2 is the experimental frequency power spectra of the SAW devices that operate with the SV and SH-SAW, respectively, in underwater environment. The SV-SAW device was fabricated on the Y-cut LiTaO$_3$ piezoelectric single crystal wafer and the SH-SAW device on the Y-cut X-propagation LiTaO$_3$ piezoelectric single crystal wafer. As exposed to water, the main lobe level of the SV-SAW device suffered from big attenuation while that of the SH-SAW showed little change. For stable operation of a SAW oscillator that is the most common structure of the SAW sensor, the prominent main lobe is crucial. Otherwise, the oscillation will fluctuate between the main lobe and side lobe frequencies. This experimental data confirmed the stable operation of the SH-SAW device underwater. Figure 3 shows the schematic structure of the SH-SAW device used for numerical simulation. When the SAW device with a detection layer is exposed to a protein solution, the antigens in the solution will adhere to the detection layer, which leads to mass loading on the SAW device. The effect of antigen adhesion was simplified as addition of a mass layer to the device. Figure 4 is the dispersion curve of the SH-SAW. With the increase of the layer thickness, the velocity of the SH-SAW decreased. The amount of the decrease was proportional to the sound velocity of the mass layer. Hence, measurement of the SH-SAW velocity can lead to the measurement of the adhered mass. If the thickness of the adhered mass layer is constant, measurement of the SH-SAW velocity can lead to the measurement of the density (concentration) or some other mechanical property of the adhered material. For an illustrative case, we checked the response of the SH-SAW sensor fabricated as a feedback oscillator when we placed water-drops onto the SAW delay line. The numerical and experimental results in Fig. 5 showed quite linear response of the sensor to the amount of water. This results confirmed the principle of SH-SAW sensors for characterization of protein solutions. Further analysis of the dispersion curve in Fig. 4 led to the following sensitivity equation, Eq. 1;

$$S_m = \lim_{\Delta m \to 0} \frac{1}{\Delta m} \left(\frac{\Delta v}{v} \right) \tag{1}$$

, where v is SH-SAW velocity and m is the adhered mass. The equation was utilized to obtain the sensor sensitivity in terms of the mass layer thickness and the frequency of the SH-SAW, Fig. 6. With the Fig. 6, we can determine the optimal operation frequency of the SH-SAW sensor for a constant mass layer thickness or narrow down the desired layer thickness range for a given SH-SAW frequency. For characterization of protein solutions, the immobilizer (antibody) layer and the corresponding antigen layer are deposited and adhered normally as molecular monolayers. In other words, the thickness of the mass layer in Fig. 3 are likely to be of constant thickness with known density. Therefore, the Fig. 6 is more of use for optimal design of the SAW device geometry.

3. STRUCTURE OF THE SAW SENSOR

Following the results in Sec. 2, SH-SAW sensors were fabricated on 36 degrees rotated Y-cut X-propagation LiTaO$_3$ piezoelectric single crystals in the form of twin SAW delay lines, a sensitive channel and a reference channel. Operating frequency of the sensor was 100 MHz. Each delay line of the sensor was configured as an oscillator as shown in Fig. 7. The delay line for a sensing channel was coated with a gold film on which an immobilizer layer was to be deposited to detect protein solutions. The sensing delay line was to selectively adsorb antigens when exposed to the protein solution, which would result in phase delay changes due to the mass loading effects induced by the adsorbed protein cells (antigens). The other delay line was uncoated for use as a stable reference. The relative change in the frequency of the two oscillators was monitored to measure the effects of immersion.

As confirmed in Sec. 2, the SH-SAW sensor can provide good sensitivity and system stability under liquid loading environment. However, there still was the need to optimize the sensor structure so that we could get the highest signal to noise ratio and the least energy leakage to the protein solution. For the purpose, firstly, the input IDT of the sensor was configured as a single-phase-unidirectional-transducer (SPUDT) in Fig. 8 so that most of the SAW power would be directed to the direction of the delay line. However, the directionality of the input IDT could not be perfect, and the output IDT was still bi-directional. Hence, secondly, in order to reduce the undesirable reflection of the SAW at the edges of the LiTaO$_3$ substrate, polymeric epoxy layer was attached to the bottom and the side edges of the substrate. As shown in Figure 9, the epoxy layers turned out to improve the sensor performance by attenuating undesirable reflection at the boundaries. The big reduction of the side lobe level could contribute to the more stable oscillation of the sensor. Thirdly, to secure electric stability of the antigen adhesion layer, the delay line was made to be in connection with electric ground bus of the IDT's. That connection could provide higher sensitivity and a much shorter response time as

evidenced in Fig. 10.

The optimized SAW sensor was coated with a chemical layer to immobilize protein cells. The antigen we investigated was anti-HigG and the structure of the immobilizer layer is depicted in Figs. 11 and 12. The protein A is coupled with HigG molecules to work as an immobilizer layer to hold the antigens in the protein solution to be measured. The BSA layer works as a blocking layer to prevent the adhesion of any other molecules different from the anti-HigG molecules to the SAW delay line.

4. EXPERIMENTS

Fig. 13 is the photograph of a fabricated SH-SAW sensor system consisting of the SAW sensor, an oscillator circuit and a computer system implemented with interface circuits and data display software. Placing drops of anti-HigG solution onto the sensing delay line, we observed oscillation frequency changes to investigate the response of the sensor to the mass loading effects. Fig. 14 is the representative measurement result. With the addition of more solution drops onto the sensing delay line, the sensor showed corresponding shift in its oscillation frequency. In addition, the sensor showed excellent return to its initial state when the solution drops were removed chemically from the delay line, which confirmed repeatability of the measurement. The measurement results in Fig. 15 show linear relationship between the amount of solution and the frequency shift. The same SAW sensor was also exposed to identical amount of solution but of different viscosities (different concentration of the solution). Fig. 16 shows linear dependence of the oscillation frequency shift on the viscosity as well. Hence, the sensor could measure both the mass and viscosity loading effects of the protein solution on top of its delay line in linear fashion.

5. CONCLUSIONS

We developed SH-SAW sensors to detect the properties of protein solutions. The particular protein solution tried in this work was anti-HigG solution. The developed SAW sensor showed linear response to the mass and viscosity loading effects of the solution placed on top of its delay line. The performance of the SH-SAW sensor developed in this work is quite promising in that the sensor can be applied to measurement of the properties of various protein solutions and chemical solutions while maintaining all the beauties of general SAW sensors [4].

REFERENCES

1. E. Gizeli, "Design considerations for the acoustic waveguide biosensor", *Smart Mater. Struct.* 6, 700-706, 1997.
2. W. Welsch, C. Klein, R. M. Öksüzoğlu, M. von Schickfus, and S. Hunklinger, "Immunosensing with surface acoustic wave sensors", *Sensors and Actuators A*, **62**, 562-564, 1997.
3. A. Leidl, I. Oberlack, U. Schaber, B, Mader and S. Drost, "Surface acoustic wave devices and applications in liquid sensing", *Smart Mater. Struct.* **6**, 680-688, 1997.
4. M. Hoummady, A. Campitelli and W. Wlodarski, "Acoustic wave sensor: design, sensing mechanisms and applications", *Smart Mater. Struct.* **6**, 647-657, 1997,
5. J. Du, G. L. Harding, J. A. Ogilvy, P. R. Dencher, and M. Lake, "A study of Love-wave acoustic sensors", *Sensors and Actuators A*, **56**, 211-219, 1996,
6. G. L. Harding, J. Du, P. R. Dencher, D. Barnett, and E. Howe, "Love wave acoustic immunosensor operating in liquid", *Sensors and Actuators A*, **61**, 279-286, 1997.
7. F. Josse, F. Bender, and R. W. Cernosek, "Guided Shear Horizontal Surface Acoustic Wave Sensors for Chemical and Biochemical Detection in Liquids", *Anl. Chem.* **73**, 5937-5944, 2000.
8. T. Moriizumi, and Y. unno, "New sensor in liquid using leaky SAW", *IEEE Ultrasonic Symp.*, 579-582, 1987.
9. D. W. Galipeau, P. R. Story, K. A. Vetelino and R. D. Mileham, "Surface acoustic wave microsensors and applications", *Smart Mater. Struct.*, **6**, 658-667, 1997.
10. T. Nomura, A. Saitoh, and Y. Horikoshi, "Measurement of acoustic properties of liquid using liquid flow SH-SAW sensor system", *Sensors and Actuators B,* **76**, 69-73, 2001.
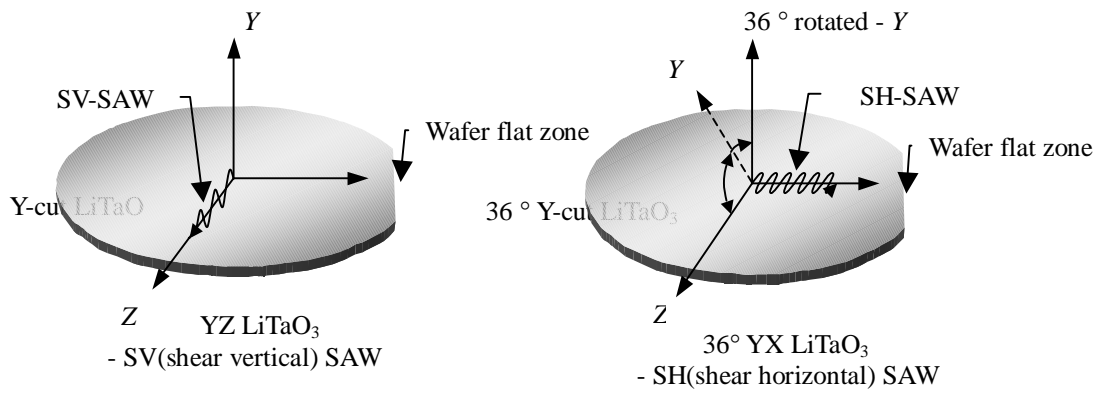
Fig. 1. Schematic diagram of SV- and SH-SAW propagation.

(a) SV-SAW device
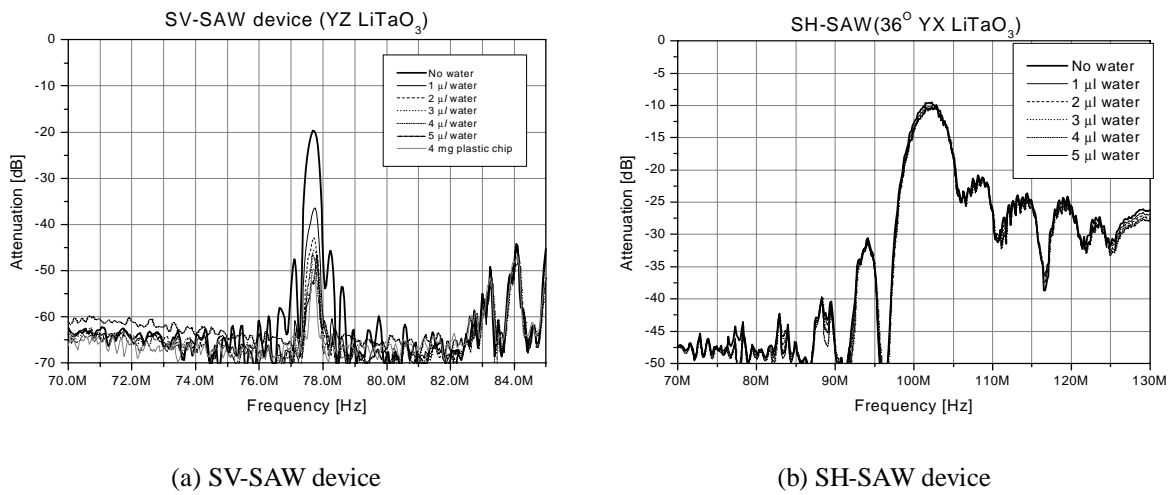
(b) SH-SAW device

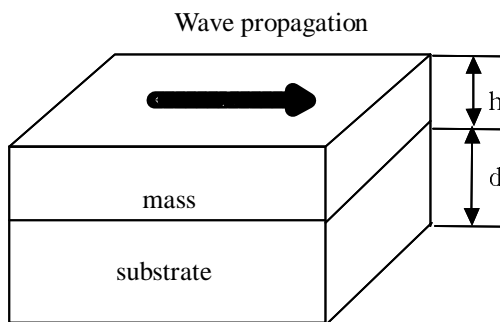Fig. 2. Power spectrum of SAW devices.

Fig. 3. Numerical analysis model
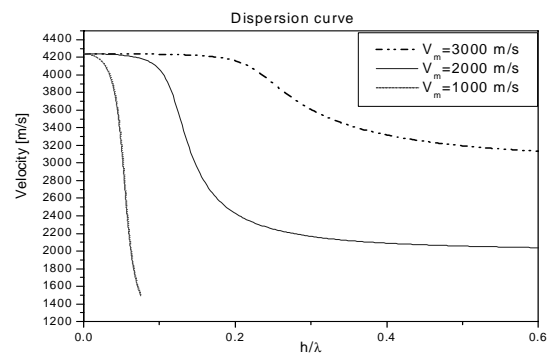
for the SH-SAW propagation.

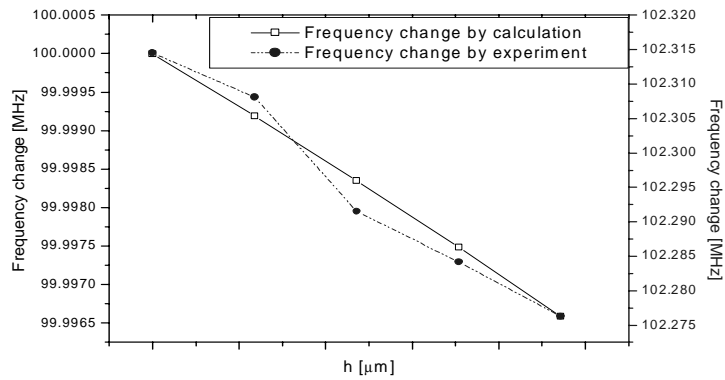Fig. 4. Dispersion curve of the SH SAW

on the layered substrate.

Fig. 5. Comparison of experimental and theoretical sensitivity
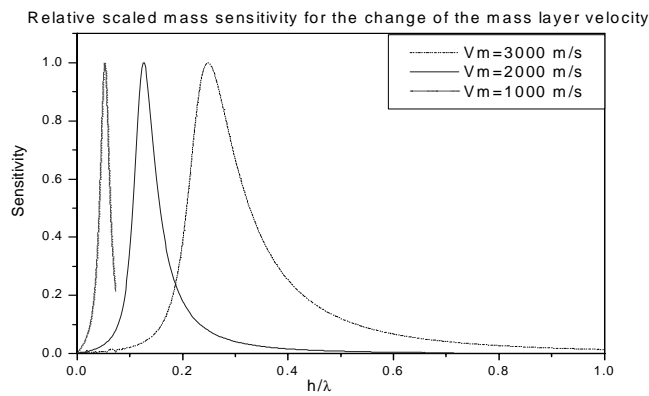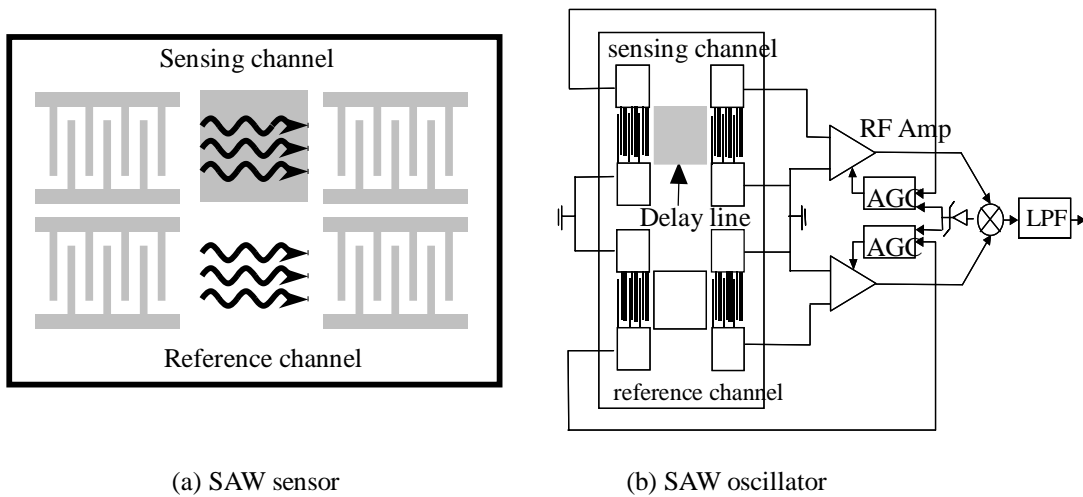of the SAW oscillator sensor in relation to the thickness of the mass layer.

Fig. 6. Mass sensitivity vs. thickness of the mass layer.

(a) SAW sensor   (b) SAW oscillator

Fig. 7. Schematic diagram of the SAW sensor.

(a) Uniform type IDT   (b) SPUDT
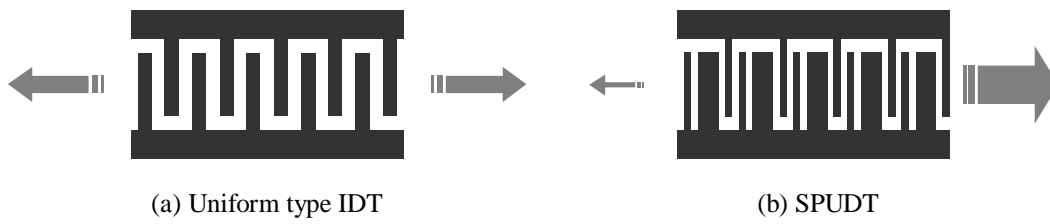
Fig. 8. Schematic configuration of the single phase unidirectional transducer (SPUDT).
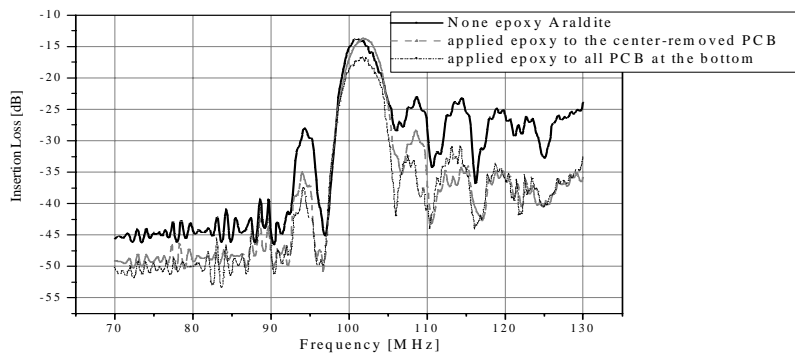
Fig. 9. Insertion loss of the sensor with different acoustic damping layer configurations.
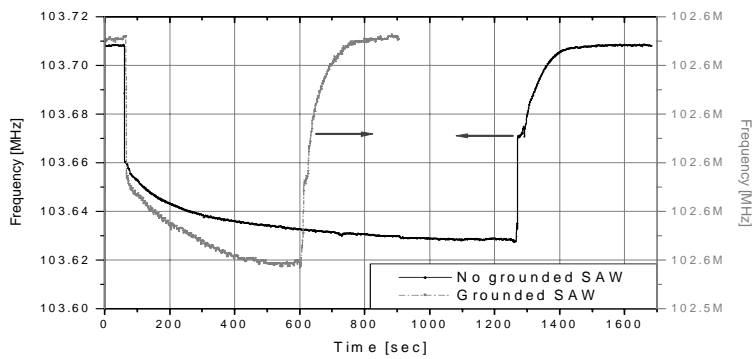
Fig. 10. Oscillation frequency change in response to water drops onto the delay line of the sensor.
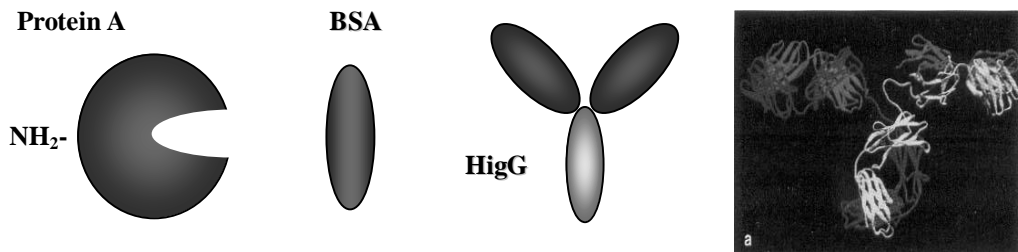
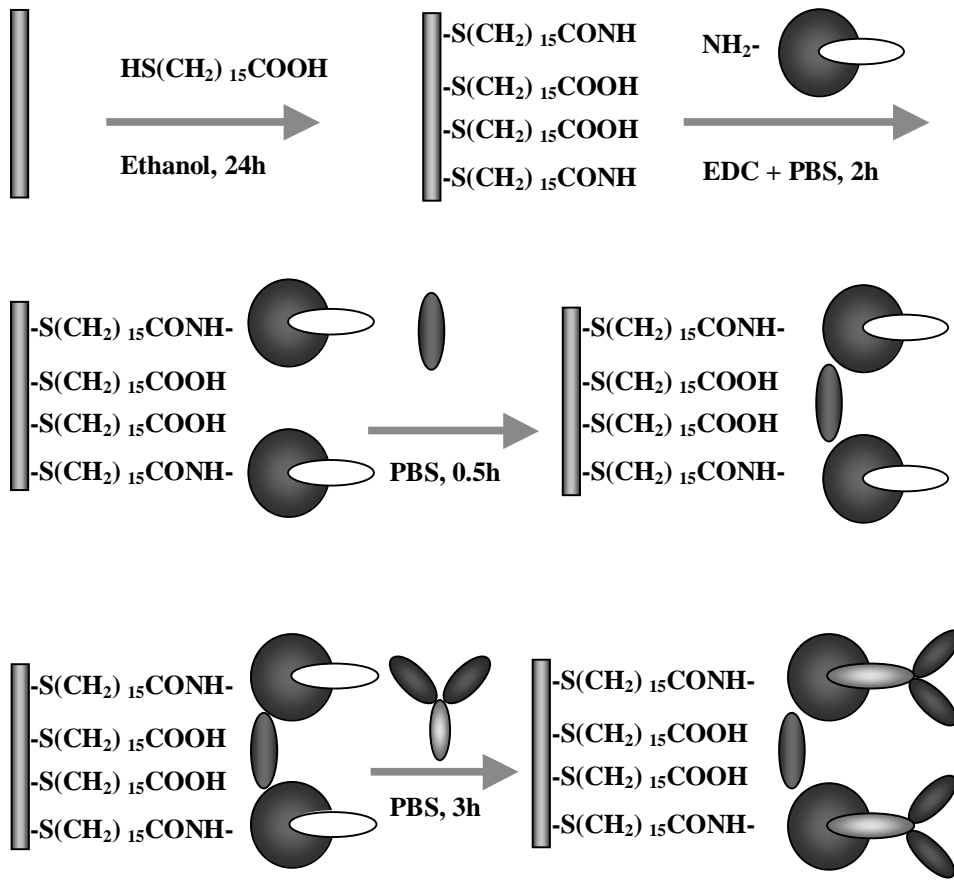Fig. 11. Elements of the immobilizer layer.
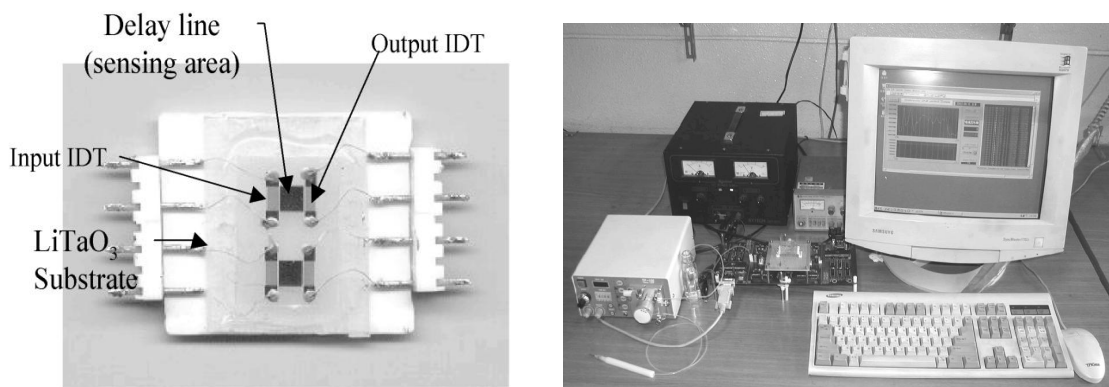
Fig. 12. The process to fabricate the immobilizer layer.

Delay line
(sensing area)

Output IDT

Input IDT

LiTaO$_3$
Substrate

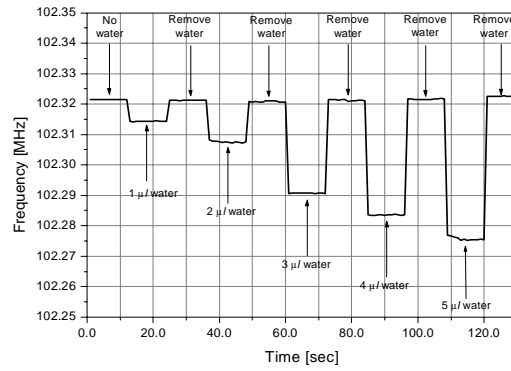Fig. 13. Complete SAW sensor system.

Fig. 14. Continuous measurement of the oscillation frequency with addition and removal of protein solution drops.
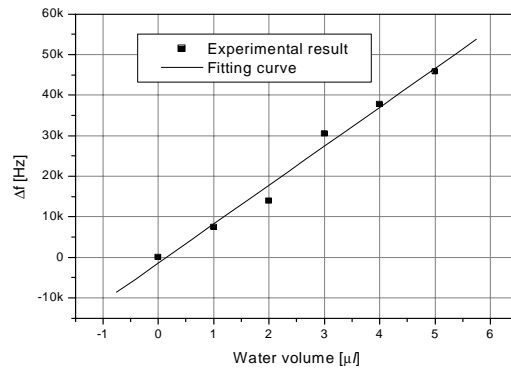

Fig. 15. Frequency shift of the SH-SAW sensor vs. volume of the protein solution.
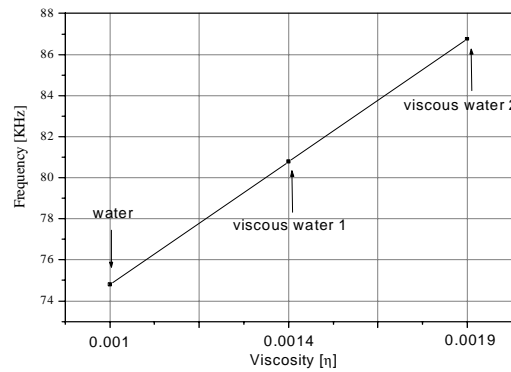

Fig. 16. Frequency shift of the SH-SAW sensor vs. viscosity of the protein solution.